

# Steam Reduction of CO<sub>2</sub> in a Photocatalytic Fluidized Bed Reactor

Vincenzo Vaiano\*, Diana Sannino, Paolo Ciambelli

Department of Industrial Engineering, University of Salerno, Via Giovanni Paolo II, 132, 84084 Fisciano (SA), Italy.  
 vvaiano@unisa.it

Unlike traditional catalysts that drive chemical reactions by thermal energy, photocatalysts can induce chemical reactions by light activation. It is well known that greenhouse gases, such as CO<sub>2</sub>, are the primary causes of global warming. From an environmental point of view, it is interesting to transform CO<sub>2</sub> into hydrocarbons, such as CH<sub>4</sub>. Since this transformation has high energy duty, a photocatalytic process can be an effective way. There are few examples in literature concerning the use of photocatalytic fluidized bed photoreactor for the reduction of CO<sub>2</sub> into CH<sub>4</sub>. The aim of this work is to investigate the performances of a high efficiency two-dimensional fluidized bed catalytic photoreactor with Cu/TiO<sub>2</sub>, Ru/TiO<sub>2</sub> and Pd/TiO<sub>2</sub>. CH<sub>4</sub> was the main product with very few amounts of CO. No deactivation phenomena were observed. Pd/TiO<sub>2</sub> photocatalysts showed the best performances. At Pd load of 1 wt. %, CH<sub>4</sub> photoproduction was 64 μmol g<sup>-1</sup> h<sup>-1</sup>, against 15 μmol g<sup>-1</sup> h<sup>-1</sup> achieved with bare TiO<sub>2</sub>. The photoreactivity reached with Pd/TiO<sub>2</sub> is significantly higher than that reported in the current literature on gas-solid photocatalytic systems for the photoreduction of CO<sub>2</sub>.

## 1. Introduction

Transition and noble metals supported on titania (TiO<sub>2</sub>) have been extensively studied as photocatalysts in several chemical reactions. Heterogeneous photocatalysis can be an effective alternative to remove bacteria (Rizzo et al., 2013) and organic pollutants such as methyl-ethyl ketone (Hajaghazadeh et al., 2014), cyclohexane (Murcia et al., 2013), methylene blue (Vaiano et al., 2014a), atrazine (Sacco et al., 2015), spiramycin (Vaiano et al., 2014b), highly polluted wastewater (Vaiano et al., 2014c) and NO<sub>x</sub> (Sannino et al., 2013b), or obtain partial oxidation products in mild conditions such as acetaldehyde (Sannino et al., 2013a) and benzene (Vaiano et al., 2014d).

Unlike traditional catalysts that drive chemical reactions by thermal energy, photocatalysts can induce chemical reactions by solar energy. It is known that greenhouse gases, such as CO<sub>2</sub>, are the primary causes of global warming. The advantage of transforming CO<sub>2</sub> into hydrocarbons, such as CH<sub>4</sub>, via photocatalytic reduction is to utilize UV or UV-visible light at low temperature and pressure. Promising photocatalysts for CO<sub>2</sub> photoreduction are Pt/TiO<sub>2</sub> (Zhang et al., 2009), Ru-TiO<sub>2</sub>/SiO<sub>2</sub> (Sasirekha et al., 2006) and Ag/TiO<sub>2</sub> (Koci et al., 2014). These photocatalysts were tested in fixed and/or batch photo-reactor, obtaining very low CH<sub>4</sub> production rates. There are no examples in literature concerning the use of a catalytic fluidized bed photoreactor for testing the reduction of CO<sub>2</sub> into CH<sub>4</sub>. In this work we have investigated the performances of such a photoreactor with different photocatalyst formulations.

## 2. Experimental

### 2.1 Catalysts preparation and characterization

Me/TiO<sub>2</sub> (Me=Cu, Ru, Pd) catalysts were prepared by wet impregnation of anatase titania (PC500, Crystal Global) with solutions of different precursor salts, followed by drying at 120°C and calcination in air at 450°C for 2 h. In particular, (C<sub>5</sub>H<sub>8</sub>O<sub>2</sub>)<sub>3</sub>Ru, CuN<sub>2</sub>O<sub>6</sub>, Pd(NH<sub>3</sub>)<sub>4</sub>(NO<sub>3</sub>)<sub>2</sub> were used for Ru/TiO<sub>2</sub>, Cu/TiO<sub>2</sub> and Pd/TiO<sub>2</sub>,

respectively. The catalysts were named xMe, where x is the nominal metal loading and Me is the metal (Cu, Ru or Pd).

Physico-chemical characterisation of catalysts has been performed with different techniques. Laser Raman spectra were obtained at room temperature with a Dispersive MicroRaman (Invia, Renishaw), equipped with 633 nm diode-laser, in the range 100-2500  $\text{cm}^{-1}$  Raman shift. UV-Vis reflectance spectra were recorded with a Perkin Elmer spectrometer Lambda 35. Equivalent band gap ( $E_{\text{bg}}$ ) determinations were obtained from Kubelka-Munk theory by plotting  $[F(R_{\infty}) \cdot h\nu]^2$  vs  $h\nu$  and calculating the x intercept of a line through  $0.5 < F(R_{\infty}) < 0.8$ . X-ray diffraction (XRD) was carried out using an X-ray microdiffractometer Rigaku D-max-RAPID, using Cu-K $\alpha$  radiation and a cylindrical imaging plate detector. Diffraction data from 0 to 204 degree horizontally and from -45 to 45 degree vertically were collected. The incident beam collimators enable different spot sizes to be projected onto the sample. Mass titration method was used to estimate the acidity of sample powders useful to measure the PZC (point zero charge) of the photocatalysts. The mass titration experiments were performed using procedures described elsewhere (Noh and Schwarz, 1989). Shorter stabilization times after each powder addition (2 h) were used to minimize possible dissolution of sample powders.

## 2.2 Photocatalytic tests

Photocatalytic tests were carried out at 140°C and atmospheric pressure, feeding 30 (stp)L/h He stream containing 1 vol. % CO<sub>2</sub>, with H<sub>2</sub>O/CO<sub>2</sub> feeding ratio in the range 0.4-4. The fluidized bed reactor used in the work was designed for working with a gas flow rate in the range 20–70 (stp)L/h and a Sauter average diameter in the particles size range 50–100  $\mu\text{m}$ , assuring optimal fluidization. It was a two dimensional reactor with 40 mm X 6 mm cross section, 230 mm height. Pyrex glass walls, and a bronze filter (mean pore size 5  $\mu\text{m}$ ) to provide a uniform distribution of fed gas. In order to decrease the amount of transported particles, an expanding section (50 mm X 50 mm cross-section at the top) and a cyclone, specifically designed are located on the top and at the outlet of the reactor, respectively. The reactor was illuminated by two UVA-LEDs modules (80X 50 mm) positioned in front of the reactor pyrex windows (UV light intensity: 90  $\text{mW cm}^{-2}$ ).

The catalyst weight was 2.2 g, diluted with of 20 g of glass spheres (grain size: 70–110  $\mu\text{m}$ ) (Lampugnani Sandblasting HI-TECH) to make easier the fluidization and to avoid a too large light absorption by the photocatalyst. In these conditions, the bed expansion is about 20%.

The outlet gas composition was continuously measured by an on-line quadrupole mass detector and a continuous CO-CO<sub>2</sub>-CH<sub>4</sub> NDIR analyser. In this way, CH<sub>4</sub>, CO<sub>2</sub> and CO were mainly detected, although other compounds were also followed in order to test the possible formation of other intermediates.

## 3. Results and discussion

### 3.1 Catalyst characterization

The Me/TiO<sub>2</sub> photocatalysts are listed Table 1. In the same Table the metal nominal loading, equivalent band gap energy, TiO<sub>2</sub> average crystallite size, and PZC values are also reported.

Table 1: Me/TiO<sub>2</sub> photocatalysts and their characteristics

Catalyst	CuO wt %	RuO <sub>2</sub> wt %	Pd wt %	$E_{\text{bg}}$ eV	TiO <sub>2</sub> average crystallites size nm	PZC pH unit
TiO <sub>2</sub>	-	-	-	3.4	7	6.6
2Cu	2	-	-	3.4	17	6.1
5Cu	5	-	-	3.0	16	5.8
10Cu	10	-	-	2.5	18	5.3
0.7Ru	-	0.7	-	2.4	13	4.4
1.7Ru	-	1.7	-	2.0	14	4.5
3.7Ru	-	3.7	-	1.9	13	4.1
0.5Pd	-	-	0.5	2.3	21	3.5
1Pd	-	-	1	2.2	25	3.4
1.5Pd	-	-	1.5	2.2	23	3.3

While TiO<sub>2</sub> nanoparticles absorb light of wavelength lower than 365 nm, after metal deposition the absorption wavelength of Me/TiO<sub>2</sub> catalysts extends to the visible region. The phenomenon becomes more evident the higher is the active phase loading.

These differences in the absorption properties corresponded to a decrease in the equivalent band gap energies with respect to bare TiO<sub>2</sub>, as shown in Table 1.

Crystal phase composition of the materials was determined by XRD measurements (Figure 1). Anatase was the only crystalline phase of TiO<sub>2</sub> identified in all samples.

No signals attributed to CuO or PdO phases were detected for 2Cu, 5Cu, 0.5Pd and 1Pd samples, due to the high dispersion and low metal content present in the materials. The catalysts with the highest Cu or Pd content showed also a small peak at about 36 and 33°, attributed to the reflection of CuO (Etefagh et al., 2013) and PdO (Mohajeri et al., 2010), respectively.

In the case of Ru/TiO<sub>2</sub> RuO<sub>2</sub> peaks at about 28° and 35° (Debecker et al., 2014) are visible for the samples 1.7Ru and 3.7Ru.

Anatase crystallite size of the catalysts was evaluated from XRD analysis, using the Scherrer equation (Table 1). For bare TiO<sub>2</sub> the anatase crystallite size was about 7 nm and increased after the active phase deposition.

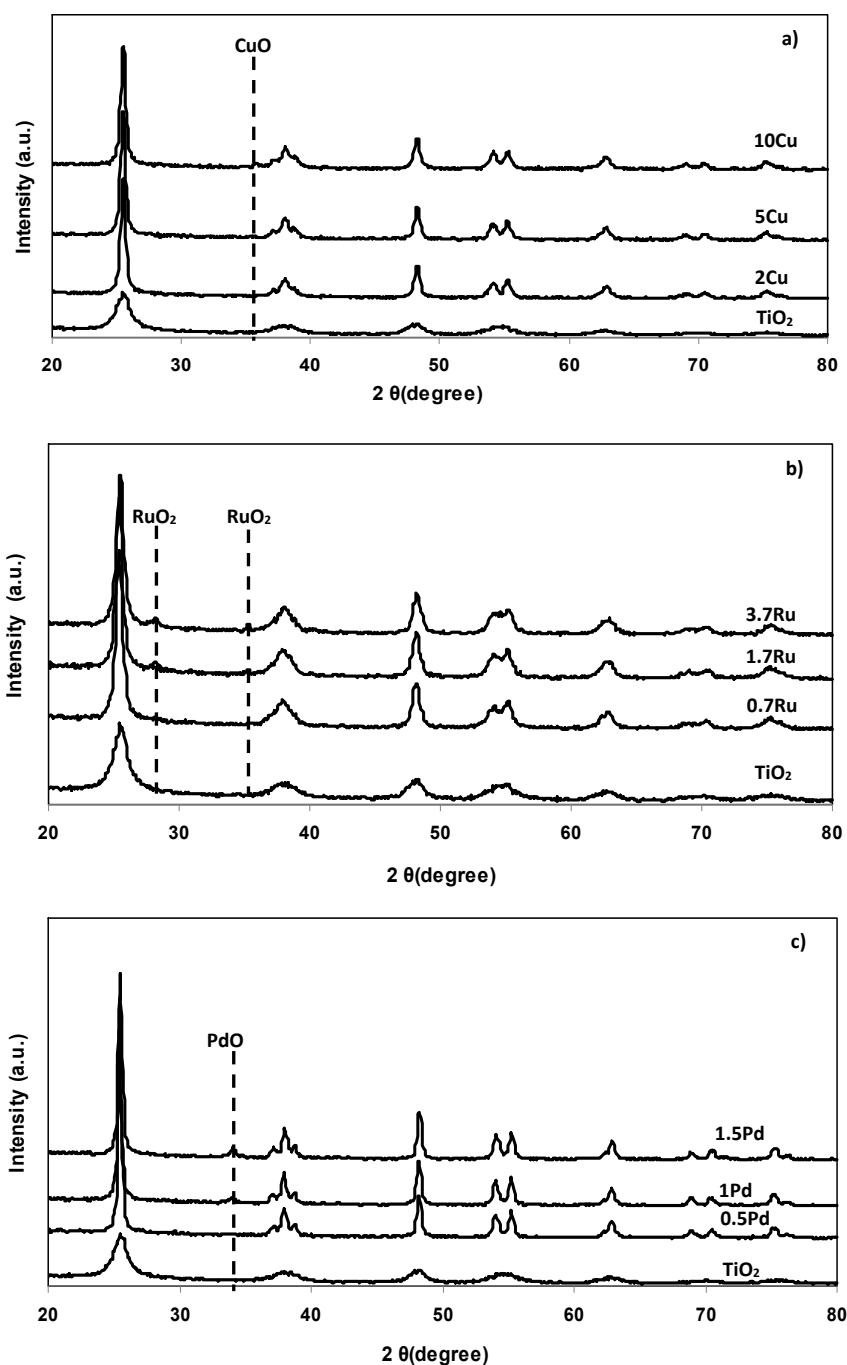


Figure 1: XRD spectra for Cu/TiO<sub>2</sub> (a), Ru/TiO<sub>2</sub> (b) and Pd/TiO<sub>2</sub> (c)

### 3.2 Photocatalytic results

Tests carried out in the absence of UV light evidenced that no reaction occurred in dark conditions.

The UV-irradiation of photocatalysts in the presence of a mixture of CO<sub>2</sub> and H<sub>2</sub>O led to the evolution of CH<sub>4</sub> as main product, as well as trace amounts of CO. No deactivation phenomena were observed during the irradiation time.

The influence of H<sub>2</sub>O/CO<sub>2</sub> feeding ratio on methane formation rate is reported in Figure 2.

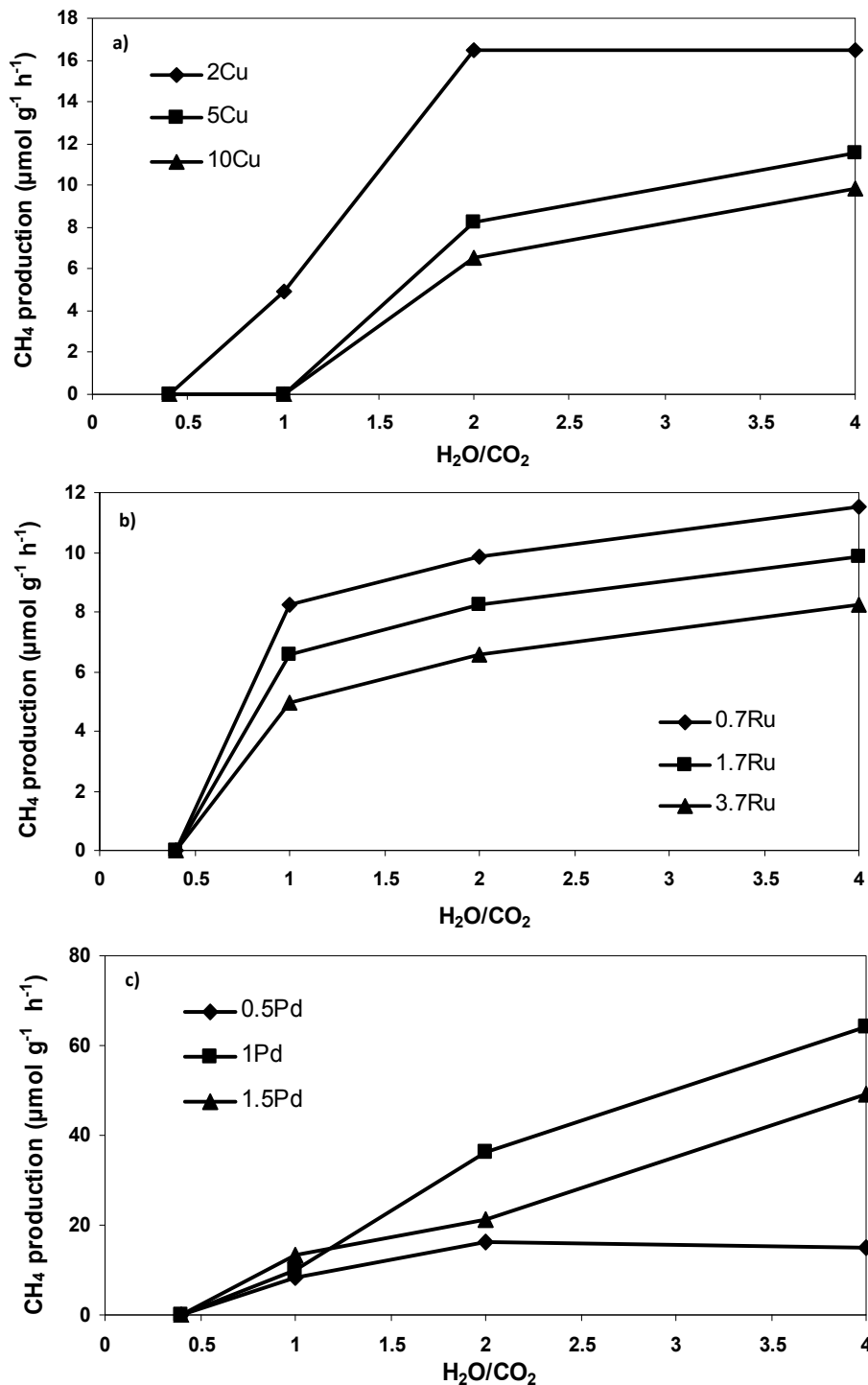


Figure 2: Influence of H<sub>2</sub>O/CO<sub>2</sub> feeding ratio on methane production for Cu/TiO<sub>2</sub> (a), Ru/TiO<sub>2</sub> (b) and Pd/TiO<sub>2</sub> (c)

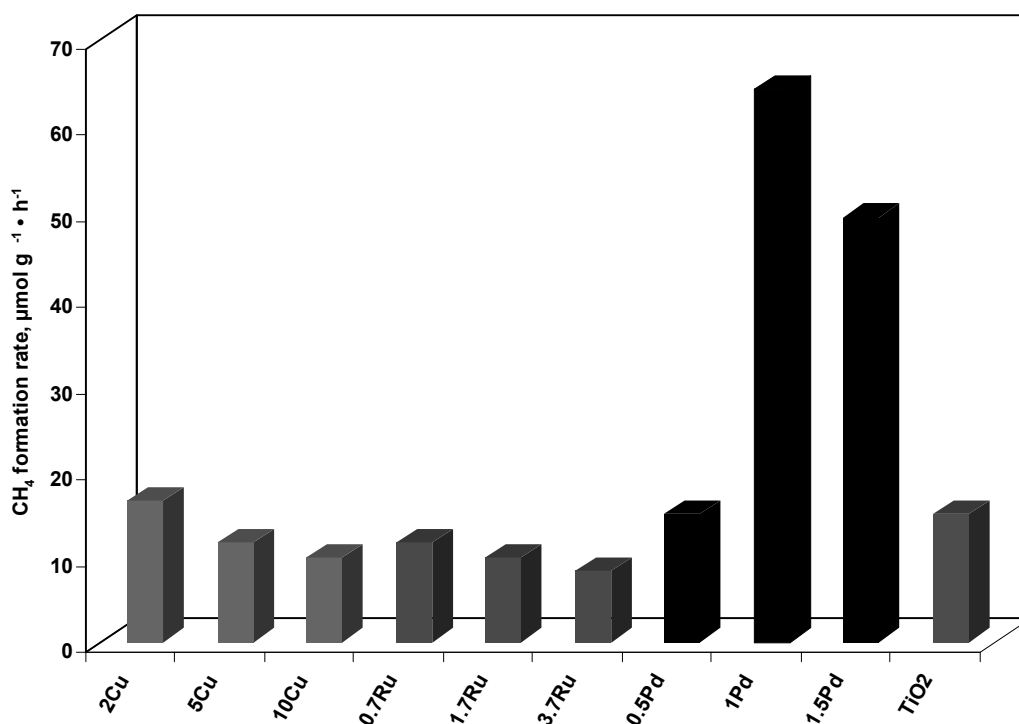


Figure 3: CH<sub>4</sub> formation rate over different photocatalysts; H<sub>2</sub>O/CO<sub>2</sub>=4

For all the tested catalysts (except for 0.5Pd sample) CH<sub>4</sub> production increased with the increase of H<sub>2</sub>O/CO<sub>2</sub> feeding ratio. At fixed H<sub>2</sub>O/CO<sub>2</sub> ratio photocatalytic activity decreased by increasing the metal loading. This last result could be explained considering that the formation of CuO, RuO<sub>2</sub> and PdO crystallites segregated on TiO<sub>2</sub> surface occurred with the increase of active phase loading, indicating a worsening of metal dispersion, as shown by XRD results (Figure 1). This phenomenon is responsible for the lowering of photocatalytic activity, as previously observed in other gas-phase photocatalytic reactions (Ciambelli et al., 2008). Figure 2 shows that the catalyst containing 1 wt% Pd yields the highest CH<sub>4</sub> production rate with respect to the others Me/TiO<sub>2</sub> samples.

The specific photocatalytic activities for the formation of CH<sub>4</sub> in the steady state conditions, for H<sub>2</sub>O/CO<sub>2</sub>=4, are summarized in Figure 3. In the case of Cu/TiO<sub>2</sub> and Ru/TiO<sub>2</sub> samples the formation of CH<sub>4</sub> was lower than TiO<sub>2</sub> alone. Moreover photo-catalytic activity decreased by increasing Cu or Ru content (as previously observed in Figure 2). The behavior was completely different when Pd was used as active phase. In this case, it is evident the existence of an optimal Pd loading. In the case of 1Pd and 1.5Pd CH<sub>4</sub> formation rate was higher than that obtained on bare TiO<sub>2</sub>, whereas on 0.5Pd photocatalyst a value very similar to TiO<sub>2</sub> was achieved. A marked increase in the CH<sub>4</sub> formation rate, up to a value of about 64 μmol g<sup>-1</sup> h<sup>-1</sup>, was found, when Pd load was equal to 1 wt.%, which is therefore the optimal active Pd loading. The photoreactivity reached on 1Pd sample is also significantly higher than that found in the current literature on gas-solid photocatalytic systems for the photoreduction of CO<sub>2</sub> (Anpo et al., 1995).

#### 4. Conclusions

Several photocatalysts active in the photocatalytic reduction of CO<sub>2</sub> to methane, were prepared and tested. Operating conditions were optimized to obtain the maximum photoreactivity in a photocatalytic fluidized bed reactor with high illumination efficiency. It was identified a class of photocatalysts based on the use of Pd supported on titania. When Pd load was equal to 1 wt. %, CH<sub>4</sub> photoproduction was 64 μmol g<sup>-1</sup> h<sup>-1</sup>, higher than that achieved with TiO<sub>2</sub> alone (about 15 μmol g<sup>-1</sup> h<sup>-1</sup>). The photoreactivity obtained with Pd/TiO<sub>2</sub> is significantly higher than that found in the current literature on gas-solid photocatalytic systems for the photoreduction of CO<sub>2</sub>. The proper formulation of the photocatalyst, together with an optimized configuration of the photoreactor, can therefore effectively allow the photocatalytic conversion of CO<sub>2</sub>, reducing the environmental impact and transforming it in chemical products with high added value in mild reaction conditions.

## References

- Anpo, M., Yamashita, H., Ichihashi, Y., Ehara, S. 1995. Photocatalytic reduction of CO<sub>2</sub> with H<sub>2</sub>O on various titanium oxide catalysts. *Journal of Electroanalytical Chemistry*, 396, 21-26.
- Ciambelli, P., Sannino, D., Palma, V., Vaiano, V., Bickley, R. I. 2008. Reaction mechanism of cyclohexane selective photo-oxidation to benzene on molybdena/titania catalysts. *Applied Catalysis A: General*, 349, 140-147.
- Debecker, D. P., Farin, B., Gaigneaux, E. M., Sanchez, C., Sasso, C. 2014. Total oxidation of propane with a nano-RuO<sub>2</sub>/TiO<sub>2</sub> catalyst. *Applied Catalysis A: General*, 481, 11-18.
- Etefagh, R., Azhir, E., Shahtahmasebi, N. 2013. Synthesis of CuO nanoparticles and fabrication of nanostructural layer biosensors for detecting *Aspergillus niger* fungi. *Scientia Iranica*, 20, 1055-1058.
- Hajaghazadeh, M., Vaiano, V., Sannino, D., Kakooei, H., Sotudeh-Gharebagh, R., Ciambelli, P. 2014. Heterogeneous photocatalytic oxidation of methyl ethyl ketone under UV-A light in an LED-fluidized bed reactor. *Catalysis Today*, 230, 79-84.
- Koci, K., Matejova, L., Reli, M., Capek, L., Matejka, V., Lacny, Z., Kustrowski, P., Obalova, L. 2014. Sol-gel derived Pd supported TiO<sub>2</sub>-ZrO<sub>2</sub> and TiO<sub>2</sub> photocatalysts; their examination in photocatalytic reduction of carbon dioxide. *Catalysis Today*, 230, 20-26.
- Mohajeri, N., T-Raissi, A., Bokerman, G., Captain, J. E., Peterson, B. V., Whitten, M., Trigwell, S., Berger, C., Brenner, J. 2010. TEM-XRD analysis of PdO particles on TiO<sub>2</sub> support for chemochromic detection of hydrogen. *Sensors and Actuators, B: Chemical*, 144, 208-214.
- Murcia, J. J., Hidalgo, M. C., Navío, J. A., Vaiano, V., Sannino, D., Ciambelli, P. 2013. Cyclohexane photocatalytic oxidation on Pt/TiO<sub>2</sub> catalysts. *Catalysis Today*, 209, 164-169.
- Noh, J. S., Schwarz, J. A. 1989. Estimation of the point of zero charge of simple oxides by mass titration. *Journal of Colloid And Interface Science*, 130, 157-164.
- Rizzo, L., Sannino, D., Vaiano, V., Sacco, O., Scarpa, A., Pietrogiamomi, D. 2013. Effect of solar simulated N-doped TiO<sub>2</sub> photocatalysis on the inactivation and antibiotic resistance of an *E. coli* strain in biologically treated urban wastewater. *Applied Catalysis B: Environmental*, 144, 369-378.
- Sacco, O., Vaiano, V., Han, C., Sannino, D., Dionysiou, D. D. 2015. Photocatalytic removal of atrazine using N-doped TiO<sub>2</sub> supported on phosphors. *Applied Catalysis B: Environmental*, 164, 462-474.
- Sannino, D., Vaiano, V., Ciambelli, P. 2013a. Photocatalytic synthesis of acetaldehyde by selective oxidation of ethanol on RuO<sub>x</sub>-VO<sub>x</sub>/TiO<sub>2</sub>. *Chemical Engineering Transactions*, 32, 625-630.
- Sannino, D., Vaiano, V., Sarno, G., Ciambelli, P. 2013b. Smart tiles for the preservation of indoor air quality. *Chemical Engineering Transactions*, 32, 355-360.
- Sasirekha, N., Basha, S. J. S., Shanthi, K. 2006. Photocatalytic performance of Ru doped anatase mounted on silica for reduction of carbon dioxide. *Applied Catalysis B: Environmental*, 62, 169-180.
- Vaiano, V., Sacco, O., Sannino, D., Ciambelli, P. 2014a. Increasing the photoactivity of N-doped TiO<sub>2</sub> photocatalysts using phosphors as light carriers. *Chemical Engineering Transactions*, 39, 619-624.
- Vaiano, V., Sacco, O., Sannino, D., Ciambelli, P. 2014b. Photocatalytic removal of spiramycin from wastewater under visible light with N-doped TiO<sub>2</sub> photocatalysts. *Chemical Engineering Journal*, 261, 3-8.
- Vaiano, V., Sacco, O., Stoller, M., Chianese, A., Ciambelli, P., Sannino, D. 2014c. Influence of the photoreactor configuration and of different light sources in the photocatalytic treatment of highly polluted wastewater. *International Journal of Chemical Reactor Engineering*, 12, 63-75.
- Vaiano, V., Sannino, D., Ciambelli, P. 2014d. Sustainable gas phase selective Photocatalytic oxidation of Cyclohexane on MoO<sub>x</sub>/TiO<sub>2</sub>/SiO<sub>2</sub> catalysts. *Chemical Engineering Transactions*, 39, 565-570.
- Zhang, Q. H., Han, W. D., Hong, Y. J., Yu, J. G. 2009. Photocatalytic reduction of CO<sub>2</sub> with H<sub>2</sub>O on Pt-loaded TiO<sub>2</sub> catalyst. *Catalysis Today*, 148, 335-340.